

# Optically trapped exciton-polariton condensates in a perovskite microcavity.

Maciej Zaremba,<sup>1,\*</sup> Mateusz Kędziora,<sup>1,\*</sup> Laura Stańco,<sup>2</sup> Krzysztof Piskorski,<sup>2</sup> Kamil Kosiel,<sup>2</sup> Anna Szerling,<sup>2</sup> Rafał Mazur,<sup>3</sup> Wiktor Piecek,<sup>3</sup> Andrzej Opala,<sup>1,4</sup> Helgi Sigurðsson,<sup>1,5,†</sup> and Barbara Pietka<sup>1,‡</sup>

<sup>1</sup>*Institute of Experimental Physics, Faculty of Physics,  
University of Warsaw, ul. Pasteura 5, PL-02-093 Warsaw, Poland*

<sup>2</sup>*Łukasiewicz Research Network - Institute of Microelectronics and Photonics, Warsaw, Poland*

<sup>3</sup>*Institute of Applied Physics, Military University of Technology, Warsaw, Poland*

<sup>4</sup>*Institute of Physics, Polish Academy of Sciences, al. Lotników 32/46, PL-02-668 Warsaw, Poland*

<sup>5</sup>*Science Institute, University of Iceland, Dunhagi 3, IS-107 Reykjavik, Iceland*

(Dated: January 29, 2025)

We demonstrate room temperature optical trapping and generation of high-order angular harmonics in exciton-polariton condensates in a monocrystalline CsPbBr<sub>3</sub> perovskite-filled microcavity. Using an annular nonresonant excitation profile focused onto the perovskite, we observed power-driven switching between different transverse modes of the optically induced trap. We explore the interplay between the perovskite crystal dimensions and the optical trap diameter that allows the condensate to transition from whispering gallery-like petal shapes to extended ripple states. Our results underline the feasibility in creating high-order quantum states in perovskite polariton condensates for reconfigurable and structured room temperature nonlinear lasing.

## I. INTRODUCTION

Exciton-polariton bosonic quasiparticles (hereafter *polaritons*) arising from the strong coupling between cavity photons and excitons, can transition into a power-driven nonequilibrium Bose-Einstein condensate displaying unconventional superfluidity and coherent light emission [1–4]. Quantum fluids of polaritons possess inherently strong optical nonlinearities due to the large Coulomb interaction strength of their exciton constituent which enables a unique optical trapping mechanism for polariton condensates [5, 6]. There, an incoherent (non-resonant) optical pump, with an annular shaped transverse beam profile, induces a polariton potential barrier at the maxima of the focused field. The effective potential originates from a photoexcited background of incoherent excitons which drive polaritons into the ring center, facilitating their stimulated scattering and condensation. Because the optically trapped condensate is mostly separated from the surrounding pumped hot region, its coherence times can increase by a factor of 10<sup>3</sup> compared to the polariton lifetime [7–9].

To date, optical trapping of polaritons has mainly been studied in inorganic cavities (e.g. CdTe and GaAs quantum wells) which, although featuring good stability under repeated excitation, require cryogenic conditions (few Kelvin) due to the small exciton binding energies. In these systems, a wide range of phenomena has been demonstrated in single traps, such as condensation into high-order modes [6, 10–15], spontaneous Larmor precession of the polariton pseudospin [7–9], Rabi cycling vortex clusters [16], polarization bifurcations [17] and bistability [18], vorticity [19, 20], tunable macroscopic Bloch

vector precession between two trap modes and associated Lotka-Volterra dynamics [21], exceptional points [22], measurement of the polariton interaction strength [23], quantum degeneracy [24], depletion [25] and Bogoliubov excitations [26]. More recently, optical traps of broken axial symmetry were rotated at GHz rates to induce preferential vorticity in polariton condensates [27–29] and probe polariton pseudospin resonances through effective magnetic fields [30].

The richness found in trapped polariton condensates, alongside their optical flexibility, has motivated researchers to explore room temperature operation using materials with much stronger exciton binding energies and light-matter Rabi coupling strength [31, 32]. For this purpose, lead halide perovskites (LHPs) are a promising candidate [33, 34] with their high optical absorption coefficients [35], tunable photon and polariton lasing [36, 37], large polariton nonlinearities [33], and relatively easy fabrication process into various microstructures [38]. Several important polariton features have already been demonstrated in perovskites such as coherent ballistic transport [39, 40], long range spin Hall currents [41, 42], analogue XY spin simulation [43], optical switches [37, 44, 45], electrically driven spin currents [46], and superfluidity [47]. However, scarce attention has been given to optically trapped polariton condensates in perovskites likely due to sample roughness which can spoil the pump-induced trap. Instead, researchers have relied on accidental sample defects [48] or irreversibly patterned structures [49–51] to trap perovskite polariton condensates. These strategies, however, do not possess the in-situ tunability that reprogrammable optical traps offer. Here, we fill in this gap by demonstrating room-temperature optical trapping of exciton-polariton condensates in microcavities containing CsPbBr<sub>3</sub> monocrystalline perovskite microwires of varying optical trap widths.

Figure 1 illustrates the fabrication process: (a) the

\* These authors contributed equally

† Helgi.Sigurðsson@fuw.edu.pl

‡ Barbara.Pietka@fuw.edu.pl

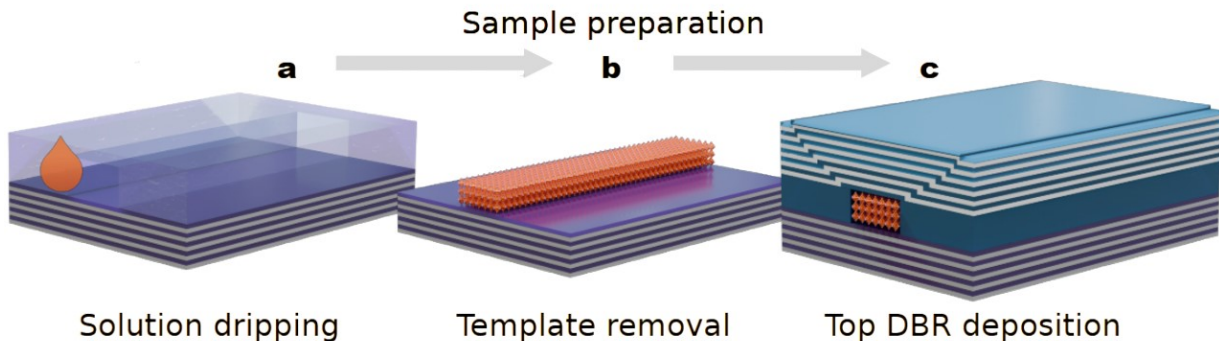


Figure 1. Sample preparation process. (a) Dripping the prepared solution in PDMS template of predefined diameter and height prepared on the 6.5 pairs of  $\text{SiO}_2/\text{TiO}_2$  DBRs' substrate. (b) Monocrystalline  $\text{CsPbBr}_3$  microwire growth by microfluidic-assisted crystallization. (c) The low-temperature PECVD technique covering with 10.5 pairs of  $\text{Si}_3\text{N}_4/\text{SiO}_2$  DBRs to obtain microcavity confinement with a photon stopband centered at 535 nm.

prepared solution was dripped into a PDMS template with predefined diameter and height, positioned on a substrate of 6.5 pairs of  $\text{SiO}_2/\text{TiO}_2$  distributed Bragg reflectors (DBRs). (b) Monocrystalline  $\text{CsPbBr}_3$  microwires were then grown using microfluidic-assisted crystallization. Following this step, the PDMS template was removed, leaving the perovskite crystals directly standing on the DBR substrate without any additional layers or covers. (c) Finally, the structure was covered with 10.5 pairs of  $\text{Si}_3\text{N}_4/\text{SiO}_2$  DBRs using a low-temperature plasma-enhanced chemical vapour deposition (PECVD) technique to achieve microcavity confinement, featuring a photon stopband centered at 535 nm. This unique fabrication technique integrates two advanced technologies critical for forming a refined high Q-factor cavity: the growth of  $\text{CsPbBr}_3$  in monocrystalline form with a precisely defined cavity thickness achieved through the predefined geometry of the PDMS template, and a top DBR mirror deposition method ensuring uniform, dense, and conformal coverage of the perovskite crystal surface.

By tailoring the LHP microwire geometry and power of the optical trap, the condensation of polaritons can be switched among different high-order trapped modes, accompanied by redistribution of spatial densities and superlinear increase in the emission intensities [see Fig. 2], implying that polariton condensates in this geometry could be exploited for an all-optical multistate switch. For low powers we observe condensation into extremely high-order angular harmonics (Laguerre-Gaussian), reminiscent of whispering gallery modes, of orbital angular quantum number up to  $l = 19$ . For higher powers we observe collapse of the condensate to successively lower order angular harmonics as stimulated scattering and phonon-mediated energy relaxation become more efficient at higher densities. For especially narrow wires (up to  $5 \mu\text{m}$ , when the standard width of microwires in the experiment is  $15 \mu\text{m}$ ) we create elongated trapping conditions which induces condensation into Hermite-Gaussian states with different mode num-

bers contrast along the minor and major trap axis, also known as *ripple* states [14]. The results underpin the potential to all-optically engineer single-particle quantum states populated by exciton-polariton condensates in LHPs.

## II. RESULTS

Our monocrystalline  $\text{CsPbBr}_3$  microwire sample of predefined diameter and height was created by microfluidic-assisted crystallization (for more details see Ref. [38]). The perovskites were first deposited on 6.5 pairs of  $\text{SiO}_2/\text{TiO}_2$  DBRs and after crystallization covered with 10.5 pairs of  $\text{Si}_3\text{N}_4/\text{SiO}_2$  DBRs at low temperature [see Fig. 1] to obtain microcavity confinement with a photon stopband centered at 535 nm. The low-temperature layers deposition (about 370 K) ensures that the perovskite structure is not disturbed, which allows to keep low the number of defects, increasing the optical quality of the structure. Even though the fabrication method of the LHP cavity is different, the final structure is similar to that described in Ref. [44].

A picosecond pulsed laser beam of  $\lambda = 435.9 \text{ nm}$  was used to nonresonantly pump the sample at large excitation densities. The ring-shaped optical trap was realized using an  $1^\circ$  axicon lens and 1 mm spatial aperture with an obstruction thickness of  $850 \mu\text{m}$  was used to eliminate residual light inside trap and provide a ring of small thickness (sub-micrometer in our case) [see Fig. 2(b)]. The profile of the pump can be described approximately by an annular Gaussian function,

$$P(r) \sim \exp\left(-\frac{(r-R)^2}{2\sigma^2}\right) + \exp\left(-\frac{(r+R)^2}{2\sigma^2}\right), \quad (1)$$

of radius  $R$  and thickness  $\sigma$ . Here,  $r = |\mathbf{r}|$  where  $\mathbf{r} = (x, y)$  is the cavity in-plane coordinate. Importantly, the experimental configuration does not impart any angular

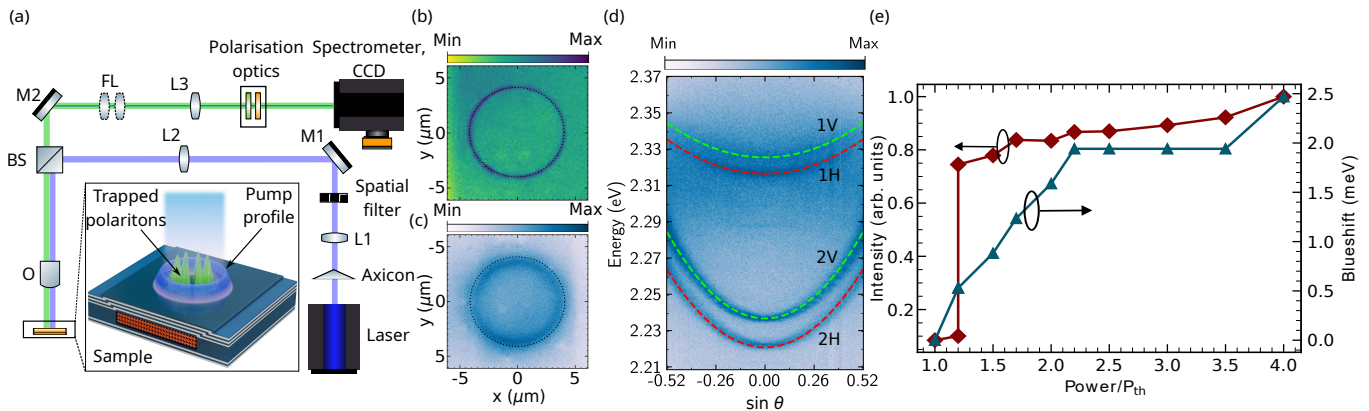


Figure 2. Experiment preparation and principal measurements. (a) A scheme of the experimental setup composed of beamsplitter (BS), objective (O), mirrors (M), lenses (L) and Fourier lenses (FL). The inset illustrates schematically the optical trap and the sample. Panel (b) shows the prepared annular laser beam profile focused on the sample and panel (c) the corresponding luminescence below threshold. The dashed circular lines help to demonstrate, as a guide-to-the-eyes, that the hot exciton reservoir is created within the pump profile. Panel (d) shows the angle resolved PL of the system below threshold, revealing two pairs of H-V (red and green curve) split polariton branches. The dashed lines are parabolic fits to the data using Eqs. (2). The data is presented in respect to the  $\sin \theta$  (where  $\theta$  is the angle at which the photoluminescence signal was collected in the experiment and  $k = E \sin \theta / \hbar c$ , where  $E$  is the polariton energy). Panel (e) demonstrates the power-dependent integrated emission intensity (red curve, arrow to the left Y-axis) and corresponding blueshift of the condensate emission line (blue curve, arrow to the right Y-axis) in units of condensation threshold power  $P_{th}$ .

momenta on the beam, and the polarization of excitation laser was vertical, the same as collected signal. Below threshold, the spatial photoluminescence (PL) pattern is mostly within the pump circumference and has a wider spread indicating exciton and polariton diffusion from the pumped region as seen in Fig. 2(c).

The LHP microwires host Wannier-Mott excitons with resonance energy centered at  $E_X = 2.375$  eV. The sample Q-factor is 340, with a characteristic photon lifetime of  $\tau \sim 100$  fs. Due to the large cavity thickness (600 nm) and birefringence, there are two pairs of horizontal (H) and vertical (V) polarization split lower-polariton energy branches within the investigated range of energies [see Fig. 2(d)]. Notably, the central energy of each pair of branches is negatively detuned from the exciton level by approximately  $\Delta \approx 55$  meV (upper pair) and  $\approx 147$  meV (lower pair). This results in two different effective polariton masses  $m_{1,2}$  which affects the dynamic condensation process of polaritons into the optical trap high order modes. For low values of  $k$  the observed polariton branches can be fitted with parabolic dispersion relations with effective masses  $m_1 = 3.8 \times 10^{-5} m_0$  and  $m_2 = 3.4 \times 10^{-5} m_0$ , where  $m_0$  represents the free electron mass. The H and V branches in each pair are also split by amount  $\epsilon_{1,2}$  attributed to the birefringence of CsPbBr<sub>3</sub> crystals [43] ( $\epsilon_1 = 35$  meV,  $\epsilon_2 = 20$  meV). The dispersion relation is expressed as:

$$\begin{aligned} E_{V1,H1} &= \bar{E}_1 + \frac{\hbar^2 k^2}{2m_1} \pm \frac{\epsilon_1}{2} \\ E_{V2,H2} &= \bar{E}_2 + \frac{\hbar^2 k^2}{2m_2} \pm \frac{\epsilon_2}{2}, \end{aligned} \quad (2)$$

where  $\bar{E}_{1,2}$  are the energies at  $k = 0$  ( $\bar{E}_1 = 1.95$  eV,  $\bar{E}_2 = 2.42$  eV).

The potential amplitude of the pump-induced annular trap is directly proportional to the density of background incoherent reservoir excitons  $n_X(r)$  which, due to their much heavier mass compared to the polariton, diffuse slowly and therefore are approximately proportional to the pump profile  $n_X(r) \sim P(r)$ . The effective polariton potential coming from many-body collisions can be written  $V(r) = 2g_0 |X_{\mathbf{k}}|^2 n_X(r)$ , where  $g_0 > 0$  is the exciton-exciton dipole interaction strength in the order of  $g_0 \sim 1 \mu\text{eV} \cdot \mu\text{m}^2$  for typical LHP [33, 34], and  $|X_{\mathbf{k}}|^2$  is the exciton Hopfield coefficient of the polariton.

Due to their low-mass photonic component, LHP cavity polaritons can coherently extend over macroscopic distances [39, 40, 47], thus making it possible for them to occupy modes over the entire optical trap. The spatial distributions of these modes can change considerably with variations in the excitation power [13, 14, 21] and microwire widths. Below the condensation threshold, polaritons are incoherent and primarily reside near the ridge of the annular pump region [see Fig. 2(c)]. When the excitation power surpasses the condensation threshold, polaritons undergo stimulated scattering into a specific trap state that provides a balance between gain and losses (similar to lasers) and not just the ground state [15]. Figures 3(a-d) show the above threshold cavity PL emanating from the annular optical trap focused within the LHP microwire. Observed condensate density profiles belong to a superposition of opposite rotating angular harmonics [10, 12–14] denoted by an orbital angular quantum index  $l = 2, 4, 15$ , and 19. Here,  $l$  is defined as the eigen-

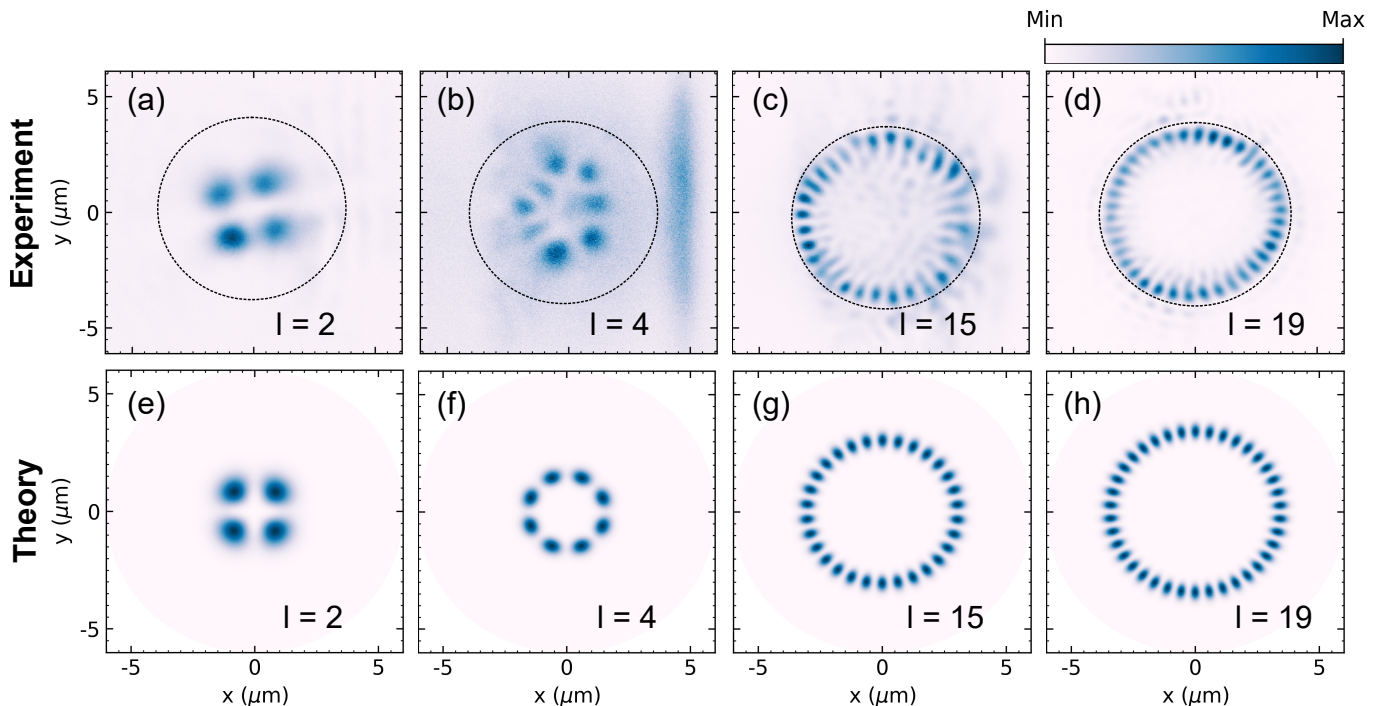


Figure 3. Optically trapped polariton condensate harmonics of varying angular momentum  $l$ . All results are resolved in V-polarization and pumped  $\approx 10\%$  above condensation threshold. The pump is centered on the microwire which is much broader. Panels (a)-(d) show the experiment, and (e)-(h) show corresponding theoretical profiles from (4). Laser profile indicated on (d) with dotted line. Condensates petals formed by ring-shaped exciton reservoirs of the spatial distribution described by (1) with different parameters for each panel, i.e. (b):  $R = 1.8 \mu\text{m}$ ,  $\sigma = 1.3 \mu\text{m}$ ; (c):  $R = 3.4 \mu\text{m}$ ,  $\sigma = 0.9 \mu\text{m}$ ; (d):  $R = 3.5 \mu\text{m}$ ,  $\sigma = 0.6 \mu\text{m}$ .

value of the angular momentum operator  $\hat{L}_z = -i\hbar\partial_\varphi$  out of the cavity plane. Different locations along the microwire sample allowed to observe different petal patterns due variable focusing of the pump profile affecting its thickness  $\sigma$ . The pump parameters for each sample location studied are given in the caption of Fig. 3(a-d). In general, the greater the pump thickness  $\sigma$  was, the lower the orbital angular momentum  $l$  observed in the condensate.

We observed that petal structures with smaller orbital angular numbers [see Fig. 3(a-c)] corresponded to condensation in the “first” 1V polariton branch [see Fig. 2(d)], whereas states with larger orbital angular numbers [see Fig. 3(d)] appear when condensation originates from the “second” 2V polariton branch. We note that H polarized emission was 10-times lower in intensity and thus negligible. The observation of polariton condensation from the different branches (1V, 2V) is linked exciton and phonon assisted relaxation of polaritons driven by the pump. For thicker pump rings [Fig. 3(a-c)], lower power densities are needed to reach threshold and thus condensation takes place in the 1V branch with polariton effective mass  $m_1$ . For narrow pump rings [Fig. 3(d)], larger power density is needed to reach threshold and thus the system is driven further out of equilibrium and collapses to the lower energy 2V branch with polariton effective mass  $m_2$ .

The observed condensate PL patterns can be fitted using the eigenstates  $|\psi_l\rangle$  of  $\hat{L}_z$  belonging to a rotationally symmetric two-dimensional harmonic confining potential:

$$\psi_l(r, \varphi) = \frac{\beta}{\sqrt{\pi l!}} e^{i l \varphi} (\beta r)^l e^{-\beta^2 r^2 / 2}. \quad (3)$$

Here,  $\beta$  is a fitting parameter denoting the strength of the “harmonic” confinement coming from the optical trap. The steady state condensate profiles correspond then to:

$$\rho(\mathbf{r}) = |\psi_{-l} + \psi_l|^2, \quad (4)$$

where  $\psi_{-l}$ ,  $\psi_l$  demonstrate two propagating polariton condensate eigenfunctions ( $\psi_l$  clockwise and  $\psi_{-l}$  counter-clockwise) inside the excitation profile, which are plotted in Fig. 3(e-h) showing good agreement. It is essential to highlight the good contrast of the measured petal shaped condensates despite operating at room temperature with broad linewidth excitons. To our knowledge, this result represents the first realization of such high-order polariton condensate states in an optical trap at room temperature. Note, the deformation of the state in Fig. 3(b) is connected with proximity of the microwire edge, also visible on the same panel as the scattered PL signal at the wire edge located along  $x = 5 \mu\text{m}$ .

We next studied the case where the pump diameter is bigger than the LHP microwire to explore finite size

effects from the wire [see Fig. (4)]. Coincidentally, at low pump powers we observe PL coming from a defect located at  $x \approx -3.5 \mu\text{m}$  [see Fig. 4(a)]. Such defects are a common issue in LHPs (for details on LHP crystal quality see Ref. [38]). As the power is increased, we eventually observe dominant emission coming from the polariton condensation populating a Hermite-Gaussian  $\psi_{n_x=1, n_y=4}$  mode [see Fig. 4(b)] with different standing wave quanta ( $n_x, n_y$ ) along  $x$  and  $y$  due to the small width of the wire compared to the pump diameter. The energy-resolved real-space PL shown in Fig. 4(c) was collected along the  $y$ -axis marked by black dotted line in Fig. 4(b). There we can see two major parts of the spectra – the PL around 2.30 eV are connected with sample defects and wire’s edges – while the much stronger and narrow lower energy PL around 2.28 eV correspond to the trapped polariton condensate. Figure 4(d) shows energy resolved cross-sections of the two states visible around 2.278 eV showing different parity.

It is also possible to tailor high-order standing wave condensates across the microwire by introducing slight eccentricity or inhomogeneity to the laser beam profile [6, 13, 14] resulting in ripple condensates shown in Figs. 5(a) and 5(b). Same as for the annular trap in Fig. 3 where 1V polaritons collapsed to 2V, when the pump power is increased the background incoherent excitons assist with the thermalization of polaritons and it starts collapsing into the trap lower excited states. We investigated this quantum-state selectivity of the condensate by performing a power scan, in units of threshold power  $P_{\text{th}}$ , where we observe the state  $\psi_{n_x=10, n_y=0}$  [Fig. 5(a) at  $1.1P_{\text{th}}$ ] smoothly transition into  $\psi_{n_x=9, n_y=0}$  [Fig. 5(b) at  $1.4P_{\text{th}}$ ]. The corresponding normalized cross sections of the condensate spatial density profiles are shown in Figs. 5(c) and 5(d). The power scan is shown in Fig. 5(e) where the number of nodes (real space interference fringes) reduces gradually at higher powers. Our findings are consistent with recent experiments in low-temperature III-V microcavity systems [21] and organic cavities [32].

### III. DISCUSSION AND CONCLUSIONS

We have demonstrated optical trapping and quantum state tailoring for exciton-polariton condensates at room temperature in CsPbBr<sub>3</sub> perovskite microcavities. Our nonresonant optical pump forms an annular ring which provides efficient transverse confinement of polaritons through their strong repulsive Coulomb interactions with a photogenerated background of hot excitons. Because of the driven-dissipative nature of the system, the observed stable condensate profiles correspond to high-order quantum states, including whispering-gallery like modes (petals) and bouncing-ball modes (ripples). The all-optical trapping aspect facilitates easy switching between these states and possible generation of complex superpositions of different states competing over the pump

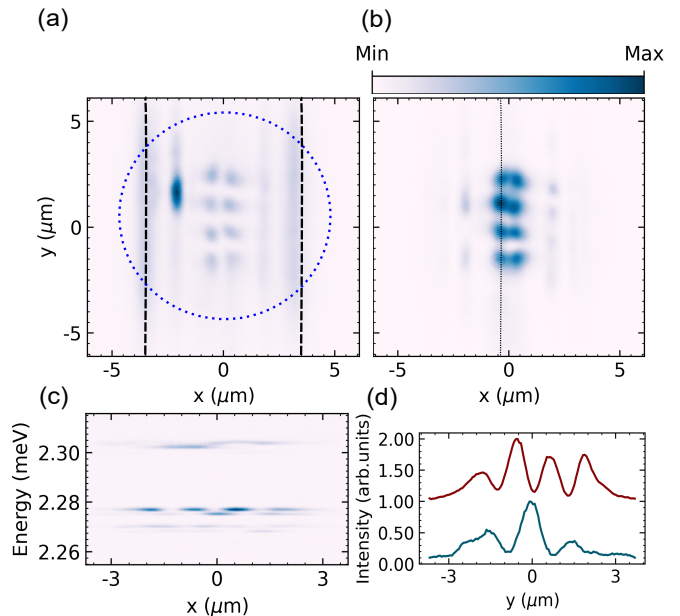


Figure 4. Asymmetric trapping of polariton condensate. Panel (a) shows emission at threshold for a situation where trap (blue dots) is bigger than wire diameter (black dashed lines). The bright emission around  $x = -3.5 \mu\text{m}$  is related to sample defect. Panel (b) is emission above (20%) threshold. Panel (c) is real space spectra taken at the same conditions as (b) and marked here by black lines. The emission around 2.3 eV is defect and edges related. Panel (d) is cross section through two states visible around 2.278 eV.

gain [21]. The patterns resemble those found in multimodal vertical-cavity surface-emitting lasers [52] and in low-temperature inorganic polariton systems [12–14]. Here, however, our perovskite system combines the advantages of all-optical reconfigurability for generation of coherent and highly nonlinear structured light with room temperature operation. Our system is also promising for future investigation into polariton condensation into high charge vortex states defined by finite net angular momenta [48]. For example, in cold atom systems, vortex formation is central to phenomena like quantum turbulence and superfluidity [53, 54]. In condensed matter physics, topologically protected vortex states emerge in systems like superconductors and superfluids, and these excitations have become important for exploring quantum phase transitions and exotic quantum states [55]. Additionally, vortex-like excitations are explored in nonlinear optics, where they are used to study the dynamics of optical beams and wavefronts, as well as their potential in quantum information processing [56, 57]. By drawing parallels between these systems and our perovskite-based polariton condensates, we open new directions for investigating topologically protected quantum states and vortex dynamics in nonlinear optical systems.

Given previous demonstrations of long-distance polaritonic propagation in microwires and waveguides [39, 40, 47] and susceptibility to engineered photonic poten-

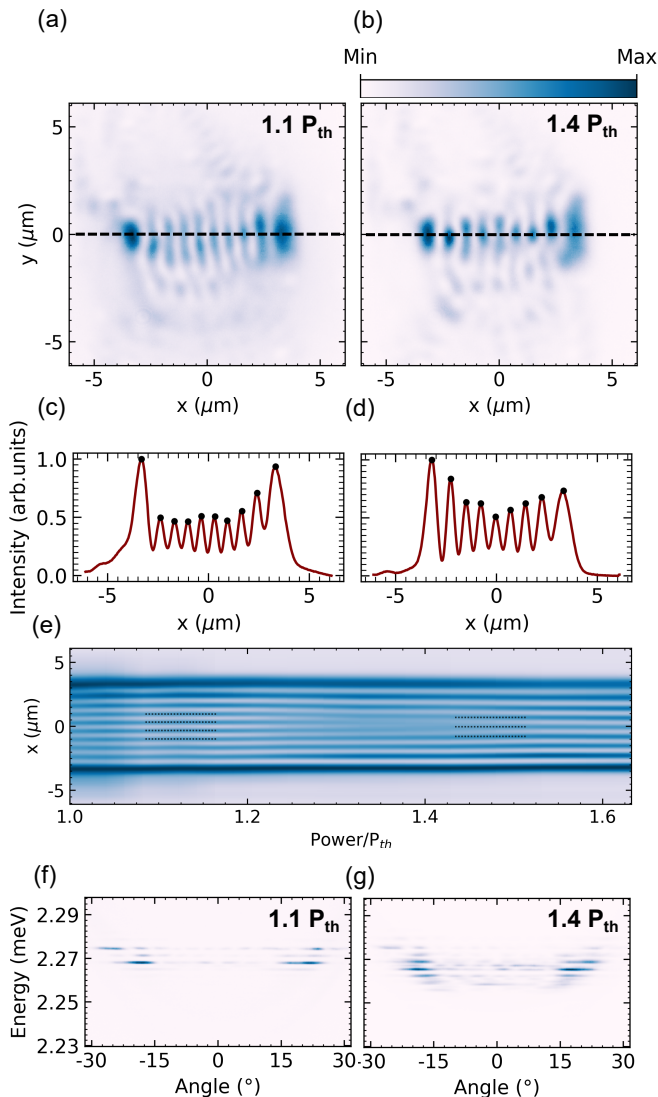


Figure 5. Tunability of mode number by pump power. Panels (a) and (b) shows real space images of trapped condensate at  $1.1$  and  $1.4 P_{th}$  using an asymmetric trap profile as indicated with blue dotted line, respectively, (c) and (d) are cross-sections of (a) and (b) at  $y = 0$  as indicated by dashed lines. Panel (e) show power-scan of the ripples number and black dotted lines are to guide the eye. The angle-resolved spectra of the condensates for pumping powers as in (a) and (b) are visible on (f) and (g). Condensate ripples formed by ring-shape exciton reservoir described by (1) with parameters:  $R = 3.4 \mu\text{m}$ ,  $\sigma = 1.5 \mu\text{m}$

tials [58], there are perspectives to combine structured optical excitation with aforementioned methods to explore new directions to control polaritons at room temperature. Already there have been demonstrations of

perovskite polaritons for optical switching in either amplitude [44, 45] or polarization [37, 42]. Another avenue involves reprogrammable condensate lattices (Fig. 5) with tunable inter-site coupling strengths through barrier height control, facilitating applications such as many-body quantum circuitry, neuromorphic and analogue optical computing and quantum simulators [59, 60]. Unconventional pump geometries, such as billiards [22] and stadiums [61], can be implemented using spatial light modulator to explore polariton chaos. Despite significant progress, challenges remain in stability, scalability, and device integration.

Another optical trapping technique worth exploring in the context of perovskites are subwavelength grating photonic structures which host negative-mass bound in the continuum polaritons that experience strong confinement under localized Gaussian pumping, instead of ring shaped pumping, with very long lifetimes [62].

## ACKNOWLEDGMENTS

M.Z. and B.P. acknowledge the European Union EIC Pathfinder Open project “Polariton Neuromorphic Accelerator” (PolArt, Id: 101130304). M.K., R.M., W.P. acknowledge the National Science Center, Poland, project No. 2022/47/B/ST3/02411. L.S., K.P., K.K. and A.S. acknowledge the support by the statutory funds of the Łukasiewicz Research Network – Institute of Microelectronics and Photonics. H.S. acknowledges the Icelandic Research Fund (Rannís), grant No. 239552-051. M.Z. and H.S. acknowledge the project No. 2022/45/P/ST3/00467 co-funded by the Polish National Science Center and the European Union Framework Programme for Research and Innovation Horizon 2020 under the Marie Skłodowska-Curie grant agreement No. 945339.

## AUTHOR CONTRIBUTIONS

M.K., B.P. and H.S. conceived the idea, M.K. grew perovskite crystals, M.Z. and M.K. performed the optical experiments, K.K., L.S, K.P. and A. S. made top DBR, R.M. and W.P. made bottom DBR, M.Z., M.K., A.O. and H.S. wrote the manuscript with input from all other authors, H.S. and B.P. supervised the project.

## COMPETING INTERESTS

The authors declare no competing interests.

[1] A. Amo, D. Sanvitto, F. P. Laussy, D. Ballarini, E. d. Valle, M. D. Martin, A. Lemaître, J. Bloch, D. N.

Krizhanovskii, M. S. Skolnick, C. Tejedor, and L. Viña, Collective fluid dynamics of a polariton condensate in a

- semiconductor microcavity, *Nature* **457**, 291 (2009).
- [2] D. Sanvitto, F. M. Marchetti, M. H. Szymańska, G. Tosi, M. Baudisch, F. P. Laussy, D. N. Krizhanovskii, M. S. Skolnick, L. Marrucci, A. Lemaître, J. Bloch, C. Tejedor, and L. Viña, Persistent currents and quantized vortices in a polariton superfluid, *Nature Physics* **6**, 527 (2010).
  - [3] T. Byrnes, N. Y. Kim, and Y. Yamamoto, Exciton-polariton condensates, *Nat. Phys.* **10**, 803 (2014).
  - [4] R. Jiggins, J. Keeling, and M. H. Szymańska, Coherently driven microcavity-polaritons and the question of superfluidity., *Nat. Commun.* **9**, 4062 (2018).
  - [5] A. Askitopoulos, H. Ohadi, A. V. Kavokin, Z. Hatzopoulos, P. G. Savvidis, and P. G. Lagoudakis, Polariton condensation in an optically induced two-dimensional potential, *Phys. Rev. B* **88**, 041308 (2013).
  - [6] P. Cristofolini, A. Dreismann, G. Christmann, G. Franchetti, N. G. Berloff, P. Tsotsis, Z. Hatzopoulos, P. G. Savvidis, and J. J. Baumberg, Optical superfluid phase transitions and trapping of polariton condensates., *Phys. Rev. Lett.* **110**, 186403 (2013).
  - [7] K. Orfanakis, A. F. Tzortzakakis, D. Petrosyan, P. G. Savvidis, and H. Ohadi, Ultralong temporal coherence in optically trapped exciton-polariton condensates, *Phys. Rev. B* **103**, 235313 (2021).
  - [8] H. Sigurdsson, I. Gnusov, S. Alyatkin, L. Pickup, N. A. Gippius, P. Lagoudakis, and A. Askitopoulos, Persistent self-induced larmor precession evidenced through periodic revivals of coherence, *Phys. Rev. Lett.* **129**, 155301 (2022).
  - [9] S. Baryshev, A. Zasedatelev, H. Sigurdsson, I. Gnusov, J. D. Töpfer, A. Askitopoulos, and P. G. Lagoudakis, Engineering photon statistics in a spinor polariton condensate, *Phys. Rev. Lett.* **128**, 087402 (2022).
  - [10] F. Manni, K. G. Lagoudakis, T. C. H. Liew, R. André, and B. Deveaud-Plédran, Spontaneous pattern formation in a polariton condensate, *Phys. Rev. Letters* **107**, 106401 (2011).
  - [11] G. Tosi, G. Christmann, N. G. Berloff, P. Tsotsis, T. Gao, Z. Hatzopoulos, P. G. Savvidis, and J. J. Baumberg, Sculpting oscillators with light within a nonlinear quantum fluid, *Nature Physics* **8**, 190 (2012).
  - [12] A. Dreismann, P. Cristofolini, R. Balili, G. Christmann, F. Pinsker, N. G. Berloff, Z. Hatzopoulos, P. G. Savvidis, and J. J. Baumberg, Coupled counterrotating polariton condensates in optically defined annular potentials, *Proceedings of the National Academy of Sciences* **111**, 8770 (2014).
  - [13] A. Askitopoulos, T. C. H. Liew, H. Ohadi, Z. Hatzopoulos, P. G. Savvidis, and P. G. Lagoudakis, Robust platform for engineering pure-quantum-state transitions in polariton condensates, *Phys. Rev. B* **92**, 035305 (2015).
  - [14] Y. Sun, Y. Yoon, S. Khan, L. Ge, M. Steger, L. N. Pfeiffer, K. West, H. E. Türeci, D. W. Snoke, and K. A. Nelson, Stable switching among high-order modes in polariton condensates., *Phys. Rev. B* **97**, 045303 (2018).
  - [15] A. V. Nalitov, H. Sigurdsson, S. Morina, Y. S. Krivosenko, I. V. Iorsh, Y. G. Rubo, A. V. Kavokin, and I. A. Shelykh, Optically trapped polariton condensates as semiclassical time crystals, *Phys. Rev. A* **99**, 033830 (2019).
  - [16] K. A. Sitnik, S. Alyatkin, J. Töpfer, I. Gnusov, T. Cookson, H. Sigurdsson, and P. G. Lagoudakis, Spontaneous formation of time-periodic vortex cluster in nonlinear fluids of light., *Phys. Rev. Lett.* **128**, 237402 (2022).
  - [17] H. Ohadi, A. Dreismann, Y. Rubo, F. Pinsker, Y. del Valle-Inclan Redondo, S. Tsintzos, Z. Hatzopoulos, P. Savvidis, and J. Baumberg, Spontaneous spin bifurcations and ferromagnetic phase transitions in a spinor exciton-polariton condensate., *Phys. Rev. X* **5**, 031002 (2015).
  - [18] L. Pickup, K. Kalinin, A. Askitopoulos, Z. Hatzopoulos, P. Savvidis, N. Berloff, and P. Lagoudakis, Optical bistability under nonresonant excitation in spinor polariton condensates., *Phys. Rev. Lett.* **120**, 225301 (2015).
  - [19] R. Dall, M. D. Fraser, A. S. Desyatnikov, G. Li, S. Brodbeck, M. Kamp, C. Schneider, S. Höfling, and E. A. Ostrovskaya, Creation of orbital angular momentum states with chiral polaritonic lenses, *Phys. Rev. Letters* **113**, 200404 (2014).
  - [20] X. Ma, B. Berger, M. Aßmann, R. Driben, T. Meier, C. Schneider, S. Höfling, and S. Schumacher, Realization of all-optical vortex switching in exciton-polariton condensates., *Nat. Commun.* **11**, 897 (2020).
  - [21] J. D. Töpfer, H. Sigurdsson, S. Alyatkin, and P. G. Lagoudakis, Lotka-Volterra population dynamics in coherent and tunable oscillators of trapped polariton condensates, *Phys. Rev. B* **102**, 195428 (2020).
  - [22] T. Gao, E. Estrecho, K. Y. Bliokh, T. C. H. Liew, M. D. Fraser, S. Brodbeck, M. Kamp, C. Schneider, S. Höfling, Y. Yamamoto, F. Nori, Y. S. Kivshar, A. G. Truscott, R. G. Dall, and E. A. Ostrovskaya, Observation of non-hermitian degeneracies in a chaotic exciton-polariton billiard., *Nature* **526**, 554 (2015).
  - [23] E. Estrecho, T. Gao, N. Bobrovska, D. Comber-Todd, M. D. Fraser, M. Steger, K. West, L. N. Pfeiffer, J. Levinsen, M. M. Parish, T. C. H. Liew, M. Matuszewski, D. W. Snoke, A. G. Truscott, and E. A. Ostrovskaya, Direct measurement of polariton-polariton interaction strength in the Thomas-Fermi regime of exciton-polariton condensation, *Phys. Rev. B* **100**, 035306 (2019).
  - [24] Y. Sun, P. Wen, Y. Yoon, G. Liu, M. Steger, L. N. Pfeiffer, K. West, D. W. Snoke, and K. A. Nelson, Bose-einstein condensation of long-lifetime polaritons in thermal equilibrium, *Phys. Rev. Lett.* **118**, 016602 (2017).
  - [25] M. Pieczarka, E. Estrecho, M. Boozarjmehr, O. Bleu, M. Steger, K. West, L. N. Pfeiffer, D. W. Snoke, J. Levinsen, M. M. Parish, A. G. Truscott, and E. A. Ostrovskaya, Observation of quantum depletion in a non-equilibrium exciton-polariton condensate, *Nat. Commun.* **11**, 429 (2020).
  - [26] M. Pieczarka, O. Bleu, E. Estrecho, M. Wurdack, M. Steger, D. W. Snoke, K. West, L. N. Pfeiffer, A. G. Truscott, E. A. Ostrovskaya, J. Levinsen, and M. M. Parish, Bogoliubov excitations of a polariton condensate in dynamical equilibrium with an incoherent reservoir, *Phys. Rev. B* **105**, 224515 (2022).
  - [27] I. Gnusov, S. Harrison, S. Alyatkin, K. Sitnik, J. Töpfer, H. Sigurdsson, and P. Lagoudakis, Quantum vortex formation in the “rotating bucket” experiment with polariton condensates., *Sci. Adv.* **9**, eadd1299 (2023).
  - [28] Y. del Valle-Inclan Redondo, C. Schneider, S. Klemmt, S. Höfling, S. Tarucha, and M. D. Fraser, Optically driven rotation of exciton-polariton condensates, *Nano Letters* **23**, 4564 (2023).
  - [29] I. Gnusov, S. Harrison, S. Alyatkin, K. Sitnik, H. Sigurdsson, and P. G. Lagoudakis, Vortex clusters in a stirred polariton condensate, *Phys. Rev. B* **109**, 104503 (2024).

- [30] I. Gnusov, S. Baryshev, H. Sigurdsson, K. Sitnik, J. D. Töpfer, S. Alyatkin, and P. G. Lagoudakis, Observation of spin precession resonance in a stirred quantum fluid of light, *Optica* **11**, 1156 (2024).
- [31] T. Guillet and C. Brimont, Polariton condensates at room temperature, *Comptes Rendus Physique* **17**, 946 (2016), polariton physics / Physique des polaritons.
- [32] M. Wei, W. Verstraelen, K. Orfanakis, A. Ruseckas, T. C. H. Liew, I. D. W. Samuel, G. A. Turnbull, and H. Ohadi, Optically trapped room temperature polariton condensate in an organic semiconductor, *Nat. Commun.* **13**, 7191 (2022).
- [33] A. Fieramosca, L. Polimeno, V. Ardizzzone, L. D. Marco, M. Pugliese, V. Maiorano, M. D. Giorgi, L. Dominici, G. Gigli, D. Gerace, D. Ballarini, and D. Sanvitto, Two-dimensional hybrid perovskites sustaining strong polariton interactions at room temperature., *Sci. Adv.* **5**, eaav9967 (2019).
- [34] R. Su, A. Fieramosca, Q. Zhang, H. S. Nguyen, E. Deleporte, Z. Chen, D. Sanvitto, T. C. H. Liew, and Q. Xiong, Perovskite semiconductors for room-temperature exciton-polaritonics, *Nat. Mater.* **20**, 1315 (2021).
- [35] R. Su, C. Diederichs, J. Wang, T. C. H. Liew, J. Zhao, S. Liu, W. Xu, Z. Chen, and Q. Xiong, Room-temperature polariton lasing in all-inorganic perovskite nanoplatelets., *Nano Lett.* **17**, 3982–3988 (2017).
- [36] Q. Zhang, Q. Shang, R. Su, T. T. H. Do, and Q. Xiong, Halide perovskite semiconductor lasers: Materials, cavity design, and low threshold, *Nano Letters* **21**, 1903 (2021).
- [37] K. Łempicka Mirek, M. Król, L. D. Marco, A. Coriolano, L. Polimeno, I. Viola, M. Kędziora, M. Muszyński, P. Morawiak, R. Mazur, P. Kula, W. Piecek, P. Fita, D. Sanvitto, J. Szczytko, and B. Piętko, Electrical polarization switching of perovskite polariton laser., *Nanophotonics* **13**, 2659 (2024).
- [38] M. Kędziora, A. Opala, R. Mastria, L. D. Marco, M. Król, K. Łempicka Mirek, K. Tyszką, M. Ekielski, M. Guzewicz, K. Bogdanowicz, A. Szerling, H. Sigurdsson, T. Czyszanowski, J. Szczytko, M. Matuszewski, D. Sanvitto, and B. Piętko, Predesigned perovskite crystal waveguides for room-temperature exciton-polariton condensation and edge lasing, *Nat. Mater.* **23**, 1476 (2024).
- [39] R. Su, J. Wang, J. Zhao, J. Xing, W. Zhao, C. Diederichs, T. C. H. Liew, and Q. Xiong, Room temperature long-range coherent exciton polariton condensate flow in lead halide perovskites, *Science Advances* **4**, eaau0244 (2018).
- [40] D. Xu, A. Mandal, J. M. Baxter, S.-W. Cheng, I. Lee, H. Su, S. Liu, D. R. Reichman, and M. Delor, Ultrafast imaging of polariton propagation and interactions, *Nature Communications* **14**, 3881 (2023).
- [41] J. Liang, W. Wen, F. Jin, Y. G. Rubo, T. C. H. Liew, and R. Su, Polariton spin hall effect in a rashba-dresselhaus regime at room temperature, *Nature Photonics* **18**, 357 (2024).
- [42] Y. Shi, Y. Gan, Y. Chen, Y. Wang, S. Ghosh, A. Kavokin, and Q. Xiong, Coherent optical spin hall transport for polaritonics at room temperature, *Nature Materials* **24**, 56 (2025).
- [43] R. Tao, K. Peng, L. Haeberlé, Q. Li, D. Jin, G. R. Fleming, S. Kéna-Cohen, X. Zhang, and W. Bao, Halide perovskites enable polaritonic xy spin hamiltonian at room temperature., *Nat. Mater.* **21**, 761–766 (2022).
- [44] J. Feng, J. Wang, A. Fieramosca, R. Bao, J. Zhao, R. Su, Y. Peng, T. C. H. Liew, D. Sanvitto, and Q. Xiong, All-optical switching based on interacting exciton polaritons in self-assembled perovskite microwires, *Science Advances* **7**, eabj6627 (2021).
- [45] R. Su, S. Ghosh, T. C. H. Liew, and Q. Xiong, Optical switching of topological phase in a perovskite polariton lattice, *Science Advances* **7**, eabf8049 (2021).
- [46] Y. Wang, G. Adamo, S. T. Ha, J. Tian, and C. Soci, Electrically generated exciton polaritons with spin on-demand, *Advanced Materials* **n/a**, 2412952 (2024).
- [47] K. Peng, R. Tao, L. Haeberlé, Q. Li, D. Jin, G. R. Fleming, S. Kéna-Cohen, X. Zhang, and W. Bao, Room-temperature polariton quantum fluids in halide perovskites, *Nat. Commun.* **13**, 7388 (2022).
- [48] X. Zhai, X. Ma, Y. Gao, C. Xing, M. Gao, H. Dai, X. Wang, A. Pan, S. Schumacher, and T. Gao, Electrically controlling vortices in a neutral exciton-polariton condensate at room temperature, *Phys. Rev. Lett.* **131**, 136901 (2023).
- [49] R. Su, S. Ghosh, J. Wang, S. Liu, C. Diederichs, T. C. H. Liew, and Q. Xiong, Observation of exciton polariton condensation in a perovskite lattice at room temperature, *Nature Physics* **16**, 301 (2020).
- [50] J. Wang, H. Xu, R. Su, Y. Peng, J. Wu, T. C. H. Liew, and Q. Xiong, Spontaneously coherent orbital coupling of counterrotating exciton polaritons in annular perovskite microcavities., *Light Sci. Appl.* **10**, 45 (2021).
- [51] L. Polimeno, A. Coriolano, R. Mastria, F. Todisco, M. De Giorgi, A. Fieramosca, M. Pugliese, C. T. Prontera, A. Rizzo, L. De Marco, D. Ballarini, G. Gigli, and D. Sanvitto, Room temperature polariton condensation from whispering gallery modes in cspbbr3 microplatelets, *Advanced Materials* **36**, 2312131 (2024).
- [52] M. Li, B. Zhang, K. P. Chen, D. W. Snoke, and A. P. Heberle, Noncircular refractive index profile and breakdown of mode degeneracy of vertical cavity surface emitting lasers, *IEEE Journal of Quantum Electronics* **48**, 1065 (2012).
- [53] C. J. Matthew, B. P. Anderson, J. R. Ensher, C. E. Wieman, and E. A. Cornell, Vortices in a bose-einstein condensate, *Physical Review Letters* **83**, 2498 (1999).
- [54] A. L. Fetter, Rotating trapped bose-einstein condensates, *Reviews of Modern Physics* **81**, 647 (2009).
- [55] W. Nernst, Zur theorie der superfluide, *Zeitschrift für Physik* **8**, 30 (1915).
- [56] G. Grosso, G. Pastori, and C. F. Rocca, Vortex dynamics in a nonlinear optical cavity, *Journal of Optics A: Pure and Applied Optics* **9**, 345 (2007).
- [57] K. Lehur, T. L. Hughes, and R. B. Laughlin, Nonlinear optics and topologically protected vortex states in photonic materials, *New Journal of Physics* **14**, 123004 (2012).
- [58] H. S. Nguyen, D. Vishnevsky, C. Sturm, D. Tanese, D. Solnyshkov, E. Galopin, A. Lemaître, I. Sagnes, A. Amo, G. Malpuech, and J. Bloch, Realization of a double-barrier resonant tunneling diode for cavity polaritons, *Phys. Rev. Letters* **110**, 236601 (2013).
- [59] A. Opala and M. Matuszewski, Harnessing exciton-polaritons for digital computing, neuromorphic computing, and optimization, *Opt. Mater. Express* **13**, 2674 (2023).
- [60] A. Kavokin, T. C. H. Liew, C. Schneider, P. G. Lagoudakis, S. Klemmt, and S. Hoefling, Polariton con-



- densates for classical and quantum computing, *Nat. Rev. Phys.* **4**, 435 (2022).
- [61] S. W. McDonald and A. N. Kaufman, Wave chaos in the stadium: Statistical properties of short-wave solutions of the helmholtz equation, *Phys. Rev. A* **37**, 3067 (1988).
- [62] A. Gianfrate, H. Sigurðsson, V. Ardizzone, H. C. Nguyen, F. Riminucci, M. Efthymiou-Tsironi, K. W. Baldwin, L. N. Pfeiffer, D. Trypogeorgos, M. De Giorgi, D. Ballarini, H. S. Nguyen, and D. Sanvitto, Reconfigurable quantum fluid molecules of bound states in the continuum, *Nature Physics* **20**, 61 (2024).